Evaluating *Eucalyptus* leaf colonization by *Brasilonema octagenarum* (Cyanobacteria, Scytonemataceae) using *in planta* experiments and genomics

Danillo O. Alvarenga[1,2], Maione W. Franco[3], Kaarina Sivonen[2], Marli F. Fiore[4] and Alessandro M. Varani[1]

[1] Departamento de Tecnologia, Faculdade de Ciências Agrárias e Veterinárias, Universidade Estadual Paulista (UNESP), Jaboticabal, São Paulo, Brazil
[2] Department of Microbiology, Faculty of Agriculture and Forestry, University of Helsinki, Helsinki, Finland
[3] Departamento de Biologia Vegetal, Centro de Ciências Biológicas e da Saúde, Universidade Federal de Viçosa (UFV), Viçosa, Minas Gerais, Brazil
[4] Divisão de Produtividade Agroindustrial e Alimentos, Centro de Energia Nuclear na Agricultura, Universidade de São Paulo (USP), Piracicaba, São Paulo, Brazil

ABSTRACT

Background. *Brasilonema* is a cyanobacterial genus found on the surface of mineral substrates and plants such as bromeliads, orchids and eucalyptus. *B. octagenarum* stands out among cyanobacteria due to causing damage to the leaves of its host in an interaction not yet observed in other cyanobacteria. Previous studies revealed that *B. octagenaum* UFV-E1 is capable of leading eucalyptus leaves to suffer internal tissue damage and necrosis by unknown mechanisms. This work aimed to investigate the effects of *B. octagenarum* UFV-E1 inoculation on *Eucalyptus urograndis* and to uncover molecular mechanisms potentially involved in leaf damage by these cyanobacteria using a comparative genomics approach.

Results. Leaves from *E. urograndis* saplings were exposed for 30 days to *B. octagenarum* UFV-E1, which was followed by the characterization of its genome and its comparison with the genomes of four other *Brasilonema* strains isolated from phyllosphere and the surface of mineral substrates. While UFV-E1 inoculation caused an increase in root and stem dry mass of the host plants, the sites colonized by cyanobacteria on leaves presented a significant decrease in pigmentation, showing that the cyanobacterial mats have an effect on leaf cell structure. Genomic analyses revealed that all evaluated *Brasilonema* genomes harbored genes encoding molecules possibly involved in plant-pathogen interactions, such as hydrolases targeting plant cell walls and proteins similar to known virulence factors from plant pathogens. However, sequences related to the type III secretory system and effectors were not detected, suggesting that, even if any virulence factors could be expressed in contact with their hosts, they would not have the structural means to actively reach plant cytoplasm.

Conclusions. Leaf damage by this species is likely related to the blockage of access to sunlight by the efficient growth of cyanobacterial mats on the phyllosphere, which may hinder the photosynthetic machinery and prevent access to some essential molecules. These results reveal that the presence of cyanobacteria on leaf surfaces is not as universally beneficial as previously thought, since they may not merely provide the

products of nitrogen fixation to their hosts in exchange for physical support, but in some cases also hinder regular leaf physiology leading to tissue damage.

INTRODUCTION

Cyanobacteria are microorganisms that colonize a wide variety of habitats, including the phyllosphere, either as free-living colonies or in symbiotic relationships. Cyanobacterial symbioses with eukaryotes are usually mutualistic, with cyanobionts providing partners with fixed carbon or nitrogen and/or defending them with toxins or sunscreens in exchange for protection from extreme environmental conditions and predation (*Usher, Bergman & Raven, 2007*; *Adams et al., 2013*; *Rikkinen, 2007*). *Brasilonema octagenarum* differs from other symbiotic cyanobacteria in this regard by presenting strains that are capable of damaging plant leaves (*Aguiar et al., 2008*), a behavior that as far as is currently known is unique in this phylum.

Thus far, *Brasilonema* strains have been found on subaerophytic habitats from tropical and subtropical environments of Brazil, French Antilles, Mexico, and USA with ten species described, namely *B. bromeliae*, *B. angustatum*, *B. burkei*, *B. geniculatum*, *B. lichenoides*, *B. octagenarum*, *B. roberti-lamii*, *B. sennae*, *B. terrestre*, and *B. tolantongensis* (*Fiore et al., 2007*; *Aguiar et al., 2008*; *Sant'Anna et al., 2011*; *Vaccarino & Johansen, 2012*; *Becerra-Absalón et al., 2013*; *Rodarte et al., 2014*; *Miscoe et al., 2016*; *Villanueva et al., 2018*; *Villanueva et al., 2019*). The distribution of the genus *Brasilonema* is most likely pantropical (*Hauer, 2010*; *Kaštovský et al., 2010*), thus new species are likely to be found in previously unsurveyed geographical regions and habitats. Nevertheless, although other strains have been isolated from the phyllospheres of different host species, plant damage has so far only been observed in *B. octagenarum*.

Ultrastructural analyses have previously shown that *B. octagenarum* UFV-E1 mats can invade the mesophylls of *Eucalyptus* leaves under nursery conditions, which results in internal cell damage and necrosis and leads to reduced rates of photosynthesis and stomatal gas exchange, eventually causing reduction in growth and harming the productivity of the host plant (*Aguiar et al., 2008*). This cyanobacterium colonized the aerial parts of *Eucalyptus* saplings and mineral substrates at the vicinity of a greenhouse (Figs. 1A–1C), with leaves colonized by strain UFV-E1 showing damage to limbs, petiole, and apical buds (Figs. 1D–1H). The molecular mechanisms by which this interaction occurs have not been elucidated yet, and whether the cellular damage is caused directly by the cyanobacterium or indirectly by its epiphytic growth is also currently unknown.

Since similar leaf damage has not been previously observed in cyanobacteria-plant interactions, it is possible that *Brasilonema octagenarum* has acquired the capacity of infecting plants from phytopathogenic organisms by horizontal gene transfer. Therefore, this work aimed to experimentally reproduce under controlled conditions the effects of *B.*
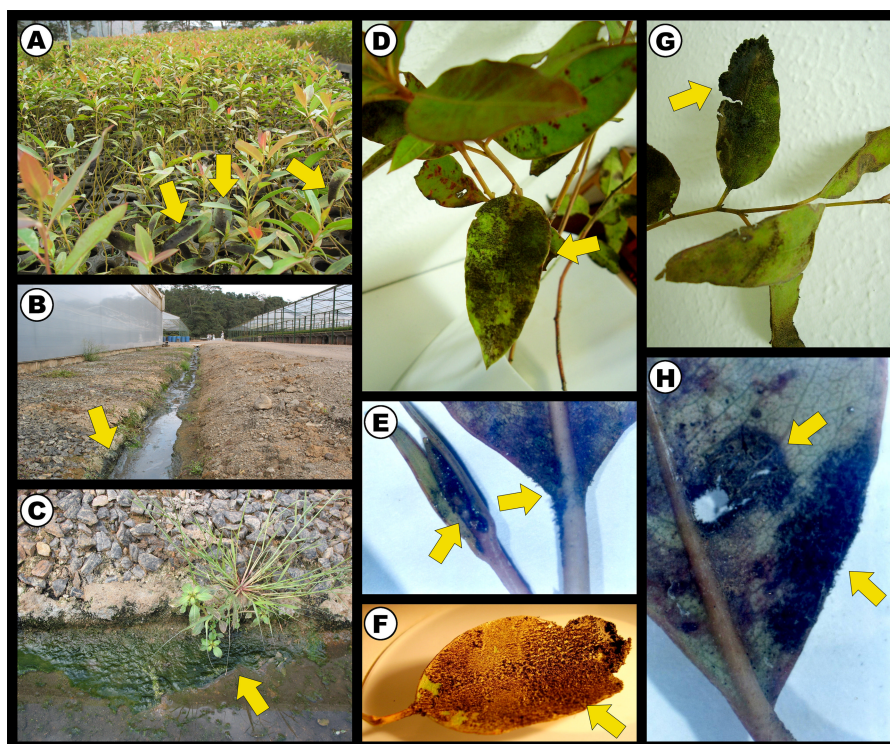
Figure 1 **Infection of *Eucalyptus urograndis* saplings by *Brasilonema octagenarum* under greenhouse conditions in Minas Gerais, southeast Brazil.** Arrows point to cyanobacterial mats. (A) *E. urograndis* nurseries presenting visible growth of *B. octagenarum* mats on leaf surfaces. (B–C) *B. octagenarum* biofilms colonizing mineral substrates in contact with water drained from a greenhouse containing *E. urograndis* plants colonized by *B. octagenarum* UFV-E1. (D–H) Limbs, petiole, and apical buds of young *E. urograndis* leaves colonized by *B. octagenarum* UFV-E1 presenting pathogenic symptoms, including necrosis. Photo credit: Maione W. Franco.

Full-size DOI: 10.7717/peerj.9158/fig-1

octagenarum UFV-E1 colonization on eucalyptus leaves; to characterize its genome to search for molecular mechanisms potentially involved in leaf damage by this strain; and to evaluate whether horizontal gene transfer had any role on the evolution of these mechanisms. For these purposes, the aerial parts of *Eucalyptus urograndis* saplings were inoculated with *B. octagenarum* UFV-E1 cultures and subsequent changes in morphology, physiology and growth of the plants were evaluated. Afterwards, the genomes of *B. octagenarum* UFV-E1 and four other *Brasilonema* spp. strains were sequenced, characterized and compared and the presence of sequences orthologous to proteins previously reported as involved in plant-pathogen interactions was inquired.

MATERIAL AND METHODS

Leaf colonization

Brasilonema octagenarum was originally found and isolated by *Aguiar et al. (2008)* in an eucalypt nursery in Minas Gerais, southeastern region of Brazil. *B. octagenarum* UFV-E1 was grown in liquid BG-11 medium (*Allen, 1968*) at temperatures of $25 \pm 2\,°C$, photoperiod

of 16/8 h light/dark and irradiance of 115 μm photons m^{-2}s^{-1}. After 30 days, the cultures were filtered using general purpose filter paper under sterile conditions and concentrated into 10% of the initial volume of 3 L to eliminate supernatants and facilitate the inoculation of leaves. Six *Eucalyptus urograndis* clonal plants were transplanted to 2 L pots containing substrate and acclimatized for two weeks in a greenhouse under the controlled conditions of 25−30 °C temperature and above 80% relative humidity. Cell suspensions were inoculated homogeneously on the aerial parts of each plant, except for six uninoculated plants used as controls. After 30 days, the cyanobacterial colonies were mechanically removed from leaf limbs using gentle fingertip movements and the middle portion of the leaves was used for extraction and quantification of pigment content. Three discs were taken from different, fresh leaves (Ø $= 0.59$ cm) in each control or inoculated plant and immersed in 7 mL of dimethylsulfoxide (DMSO) (*Wellburn, 1994*) in the dark for 24 h. Absorbance was determined at λ of 665.1, 680 and 450 for chlorophyll *a*, chlorophyll *b* and carotenoids, respectively. Stem height and leaf area were evaluated, and stem, root and leaf dry masses were measured after oven dehydration at 75 °C for 72 h. The leaf area was measured using a leaf area integrator (Delta-T Devices, Cambridge, UK). The averages of the data obtained were compared with the Tukey test (significance level $P < 0.05$) using SAS 9.2 (SAS Institute, Cary, USA).

Anatomical evaluation

Leaf blade samples collected from inoculated and control plants were fixed with 50% FAA solution (formaldehyde, acetic acid and 70% ethanol) for 48 h and stored in 70% ethanol (*Johansen, 1940*). After the middle blade region was sectioned and the samples were embedded in Histosec (Merck, Kenilworth, USA), 10 μm cross sections were obtained with an automatic advance rotary microtome. Part of the cuts were stained with safranin/astra blue (*Bukatsch, 1972*) for observing the general structure and presence of phenolic compounds, and the other part was stained with scarlet Sudan (*Sass, 1951*) for cuticle observation. Next, the cuts were mounted on Permount synthetic resin (Thermo Fisher Scientific, Waltham, USA). Sections were examined and images were captured with the Olympus AX-70 photomicroscope system (Olympus, Shinjuku, Japan) using the Image-Pro Discovery software (MediaCybernetics, Silver Spring, USA).

High-throughput sequencing

Brasilonema octagenarum UFV-E1, *B. octagenarum* CENA114, *B. octagenarum* UFV-OR1, *B. bromeliae* SPC 951 and *Brasilonema* sp. UFV-L1 were grown as non-axenic, unicyanobacterial cultures in 125 mL Erlenmeyer flasks containing 50 mL of sterile BG-11$_0$ liquid medium (*Allen, 1968*; *Stanier et al., 1971*). For the reduction of associated microbes, the samples were washed with ultrapure water, 0.05% Extran, 0.85% NaCl, and a solution composed of 50 mM NaCl, pH 7.5 10 mM Tris-HCl and pH 8.0 2.5 mM EDTA. After inoculation, incubation was carried out at 25 $\pm$ 1 °C with a photoperiod of 14 h of light and 10 h of darkness under fluorescent light of 40 μmol photons m^{-2} s^{-1}. Two-week-old cultures were centrifuged for 10 min at 7,690$\times$ g and cells were collected for DNA extraction using a modified version of the protocol established by *Lin et al. (2010)*.

Paired-ends libraries were produced for all strains with the Nextera XT DNA Sample Prep Kit (Illumina) according to manufacturer's instructions. Additionally, mate-paired libraries were prepared from 8 kbp inserts for strains UFV-E1 and CENA114 using the Nextera Mate Pair Library Prep Kit (Illumina) according to the manufacturer's protocols in order to improve assemblies and obtain complete genomes for the main strain of this study and the strain not isolated from phyllosphere. Sequencing was carried out in the HiSeq 2500 platform using the HiSeq v4 Reagent Kit (Illumina) following the instructions provided by the manufacturer.

Genome assembly

Bases with qualities lower than Phred 28, adapters and sequences shorter than 50 bp were removed from the datasets with Trimmomatic 0.36 (*Bolger, Lohse & Usadel, 2014*). Mate-paired libraries were further refined with NxTrim 0.4.2 (*O'Connell et al., 2015*) for the separation of true mate-paired reads. *De novo* assemblies were carried out using SPAdes 3.11.1 (*Bankevich et al., 2012*) and MaSuRCA 3.2.4 (*Zimin et al., 2013*). Kraken 1.0 (*Wood & Salzberg, 2014*) and MetaBAT 2.12.1 (*Kang et al., 2015*) were used for identifying cyanobacterial sequences among the assembled contigs. Platanus 1.2.4 (*Kajitani et al., 2014*) was used for further scaffolding and gap closing. Genome completeness and contamination were estimated with CheckM 1.0.7 (*Parks et al., 2014*).

Genome annotation

The assembled genomes were automatically annotated with the NCBI Prokaryotic Genome Annotation Pipeline (*Tatusova et al., 2016*). When necessary, manual curation of annotations was performed with Artemis 16.0.17 (*Carver et al., 2012*) and BLAST 2.6.0+ (*Camacho et al., 2009*). Functional identification of translated protein sequences into orthologous groups was performed with eggNOG 4.5.1 (*Huerta-Cepas et al., 2016*), Blast2GO 5.2 (*Götz et al., 2008*) and WEGO (*Ye et al., 2018*). The RAST server (*Overbeek et al., 2014*; *Brettin et al., 2015*) was used for predicting the subsystems present in the assembled genomes. Protein sequences from the Pathogen-Host Interactions Database version 4.5 (*Urban et al., 2020*) were used to uncover genes encoding proteins similar to known virulence factors by using TBLASTN with cut-off values of 90% for coverage and 60% for positive-scoring amino acid matches. Translated protein sequences for hypothetical proteins were retrieved from the assembled genomes and their domains were predicted with the Phobius web server (*Käll, Krogh & Sonnhammer, 2007*). Predictions for possible effectors from the type III secretion system were performed with the EffectiveDB web server (*Eichinger et al., 2016*).

Prediction of mobile genetic elements

The occurrence of mobile genetic elements in the genomes obtained was verified according to the protocols described in *Alvarenga et al. (2018)*. Insertion sequences were predicted with OASIS 8/11/08 (*Robinson, Lee & Marx, 2012*), ISEScan 1.5.4.3 (*Xie & Tang, 2017*) and the ISfinder database (*Siguier et al., 2006*; *Siguier et al., 2012*). Prophages were predicted with PhiSpy 3.2 (*Akhter, Aziz & Edwards, 2012*) and VirSorter 1.0.3 (*Roux, Enault & Hurwitz, 2015*). CRISPRs were detected with MinCED 0.2.0

(https://github.com/ctSkennerton/minced). For the uncovering of genomic regions with anomalous content, Alien_Hunter 1.7 (*Vernikos & Parkhill, 2006*), OligoWords 1.2.1 and SeqWord Sniffer 2.0 (*Ganesan et al., 2008*) were used.

Genome comparisons and phylogenomic analyses

OrthoANIu 1.2 (*Yoon et al., 2017*) and USEARCH 10.0.240 (*Edgar, 2010*) were used for estimating average nucleotide identity among the assembled genomes. Orthologous protein clusters shared among the strains were surveyed by the OrthoVenn server (*Wang et al., 2015*). The assembled genomes were included in a dataset with 154 complete and nearly complete cyanobacterial genomes retrieved from the NCBI RefSeq database (*O'Leary et al., 2016*) for selection of marker sequences with Metaxa 1.0.2 (*Bengtsson et al., 2011*) and Phyla-AMPHORA 03/19/13 (*Wang & Wu, 2013*). Multiple sequence alignments for sixty single-copy translated protein sequences shared by all genomes and 16S rRNA gene sequences were produced with MAFFT 7.309 (*Katoh & Standley, 2013*) and concatenated into a single alignment. A maximum likelihood phylogenomic tree was reconstructed from the concatenated translated proteins/16S rRNA gene alignment with RAxML 8.2.9 (*Stamatakis, 2014*) using the best-fit evolutionary models for each partition as calculated with the phylogenomics-tools pipeline (https://github.com/kbseah/phylogenomics-tools). The tree was visualized with FigTree 1.4.2 (http://tree.bio.ed.ac.uk/software/figtree/) and edited with Inkscape 0.92 (https://inkscape.org/).

RESULTS

Eucalyptus leaf inoculation

We first reinoculated *B. octagenarum* strain UFV-E1 on *E. urograndis* leaves to check if the cyanobacterial colonization and its effects previously found under natural conditions could be artificially replicated on seedlings. One month after inoculation, *E. urograndis* leaves colonized by strain UFV-E1 showed a significant decrease of 19% in the Chl *a*/Chl *b* ratio in the areas colonized by the cyanobacterium (Table 1). When the content of the pigments Chl *a*, Chl *b* and carotenes were analyzed individually, significant alteration in the colonized areas in relation to the control samples was not verified (Table 1). The inoculated plants had an increase in root and stem dry mass (19% and 23%, respectively) and stem height (7%), while leaf dry mass and area showed no significant differences between inoculated plants and controls (Table 2).

 B. octagenarum UFV-E1 colonized *E. urograndis* blades at points scattered along leaf surfaces (Figs. 2A and 2B). After the removal of the cyanobacterial colonies (Fig. 2C), the regions previously covered by denser colonies showed alterations in pigmentation (Fig. 2D). Transverse sections of *E. urograndis* leaves from the control group showed a prominent central rib on the abaxial face, presenting a bicollateral vascular bundle on both sides and fundamental parenchyma (Fig. 3A). The epidermis was unstratified, covered by cuticle, showing stomata mainly on the abaxial face. The mesophyll was dorsinventral, composed of palisade parenchyma formed by one or two layers of cells, and lacunar parenchyma, formed by three or four layers (Fig. 3B). In the plants colonized by *B. octagenarum*, colonies were observed mainly on the adaxial face (Figs. 3C and 3D). No structural changes were

Table 1 Pigment content in leaf areas of *Eucalyptus urograndis* plants colonized by *Brasilonema octagenarum*. *Significant effect at $P \leq 0.05$, Tukey test.

Sample	Chl *a* ($\mu g\,cm^{-2}$)	Chl *b* ($\mu g\,cm^{-2}$)	Carotenoids ($\mu g\,cm^{-2}$)	Chl *a/b**
controls	15.64 ± 0.47	6.78 ± 0.29	2.98 ± 0.21	2.32 ± 0.10
inoculated plants	14.45 ± 0.44	7.42 ± 0.33	2.93 ± 0.30	1.95 ± 0.06

Table 2 Growth variables evaluated in *E. urograndis* plants after inoculation with *B. octagenarum*. Significant effects at * $P \leq 0.05$ and ** $P \leq 0.01$, Tukey test.

| Sample	Root dry weight (g)	Stem dry weight (g)	Leaves dry weight (g)	Leaf area (cm^2)	Stem height (cm)
controls	$15.11^* \pm 0.63$	$23.07^{**} \pm 1.01$	21.22 ± 1.82	$3,586.5 \pm 255.3$	$83.3^{**} \pm 1.3$
inoculated pants	17.94 ± 0.73	28.36 ± 0.99	22.47 ± 0.49	$4,136.5 \pm 147.5$	89.5 ± 1.2

observed caused by colonization (Fig. 3C) in the regions of the central rib or the remainder of the leaf lamina (Fig. 3D). The cuticle remained without changes in the regions colonized by *B. octagenarum* (Figs. 3F and 3G) in comparison with the controls (Figs. 3E and 3G).

Genomic sequencing and characterization

The genome sequencing of *Brasilonema* strains resulted in the assembly of nearly complete genomes for *B. octagenarum* UFV-E1 and *B. octagenarum* CENA114 while draft genomes were obtained for *B. octagenarum* UFV-OR1, *B. bromeliae* SPC 951 and *Brasilonema* sp. UFV-L1 (Fig. 4A, Table 3). The genome sequences obtained in this work were deposited in the NCBI Genome database under the accession numbers CP030118–CP030123, QMEA00000000, QMEB00000000, QMEC00000000. Predictions for the nearly complete chromosomes of strains UFV-E1 and CENA114 uncovered 17 and 14 genome islands, respectively. Additionally, 158 insertion sequences were found in both sequences. No prophages were detected in those chromosomes. On the other hand, two remnant prophage regions were predicted in each plasmid from both strains. Except for the UFV-E1 190 kbp plasmid, two genome islands were also detected in those plasmids. Moreover, 11 additional insertion sequences were found in the 250 kbp plasmids, while 18 and 16 insertion sequences were detected in the 190 kbp plasmids from UFV-E1 and CENA114, respectively. Finally, 9 CRISPR loci were predicted in both nearly complete chromosomes. Average nucleotide identity (ANI) among strains UFV-E1, CENA114, and UFV-OR1 was calculated as 99%, showing that they are actually representatives of the same species, *B. octagenarum*, which presented 90 and 85 ANI percentages when their genomes were compared to the genomes of *B. bromeliae* SPC 951 and *Brasilonema* sp. UFV-L1, respectively (Fig. 4B). Clustering analyses revealed a large number of orthologous protein clusters shared among the analyzed *Brasilonema* genomes, with a very small amount of protein clusters exclusive to each strain (Fig. 4C).

In the virulence, disease and defense subsystem predicted in the nearly complete *B. octagenarum* genomes, genes involved in resistance to fluoroquinolone- and betalactam-based antibiotics were found, in addition to genes for resistance to copper, mercury, arsenic,
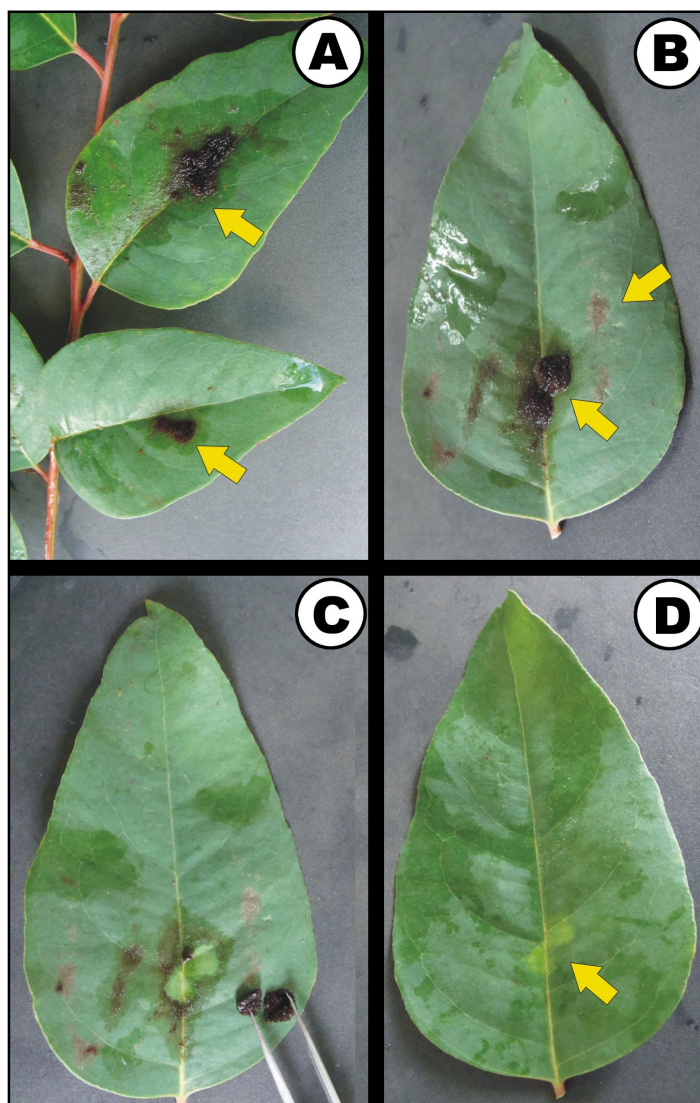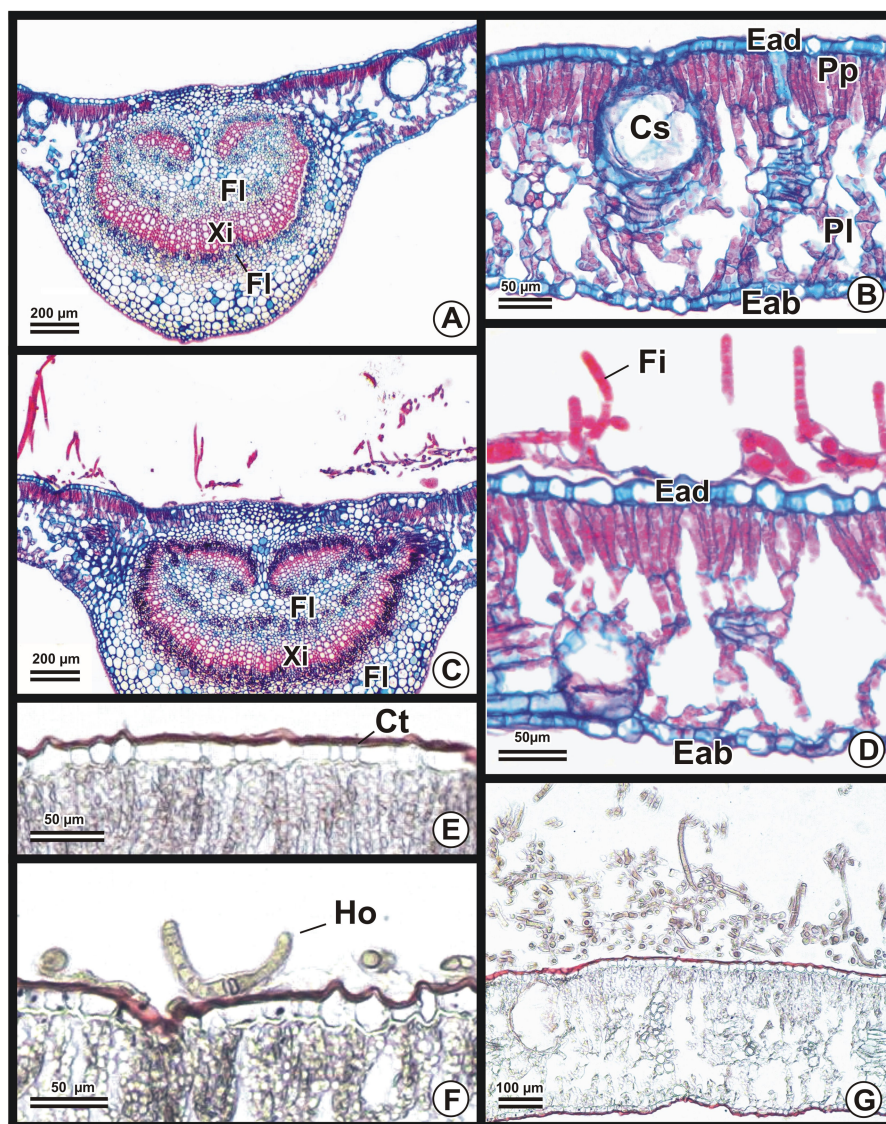
Figure 2 *Eucalyptus urograndis* **leaves colonized by** *Brasilonema octagenarum* **UFV-E1.** (A) General appearance of colonized leaves presenting conspicuous growth of cyanobacterial filaments. (B) Cyanobacterial mats covering the central vein of the host leaf. (C) Removal of cyanobacterial colonies from the leaf surface. (D) Discoloration in leaf areas previously covered by cyanobacterial colonies. Photo credit: Maione W. Franco.

Full-size 🖻 DOI: 10.7717/peerj.9158/fig-2

chromium and cobalt/zinc/cadmium, suggesting that these cyanobacteria may have some tolerance to environmental disturbances, such as contamination by toxic element. However, subsystem coverage was very low in the assembled genomes, as merely 18% of sequences in the *B. octagenarum* genomes could be included into known subsystems, while subsystem coverage in the *B. bromeliae* SPC 951 and *Brasilonema* sp. UFV-L1 genomes amounted to 17% of their content. Similarly, the most abundant functional categories for clusters of orthologous groups (COGs) in all genomes were those with general function prediction only or unknown function. Overall all strains presented very similar number of genes

Figure 3 Photomicrographs of cross sections from *Eucalyptus urograndis* leaves stained with safranin/astra blue (A–D) or Sudan (E–G). (A) Cross section of a control leaf, showing the xylem (Xy) and phloem (Fl) in a general view of its central rib. (B) Portion of a control leaf blade in higher magnitude, showing more details of the epidermis of the adaxial (Ead) and abaxial (Eab) surfaces, a secretory cavity (Cs), the palisade parenchyma (Pp) and the lacunar parenchyma (Pl). (C) Central rib colonized by *Brasilonema octagenarum*, with filaments on the adaxial side of the epidermis. (D) Portion of the leaf lamina evidencing the fasciculate growth pattern of the cyanobacterial filaments (Fi) on the adaxial surface. (E) Control leaf epidermis showing a red-orange cuticle (Ct). (F) Integral cuticle in inoculated plants, evidencing an hormogonium (Ho). (G) Portion of the colonized leaf blade, presenting a dense layer of filaments of *B. octagenarum* on the adaxial side with an intact cuticle. Photo credit: Maione W. Franco.

Full-size ⤢ DOI: 10.7717/peerj.9158/fig-3

related to known COG and GO terms (Fig. 5, Table S2), suggesting that these species may perform similar ecological roles. The analysis of translated protein sequences from genes annotated as encoding hypothetical proteins with the Phobius webserver revealed that roughly three quarters are likely non-cytoplasmic and approximately one quarter of these
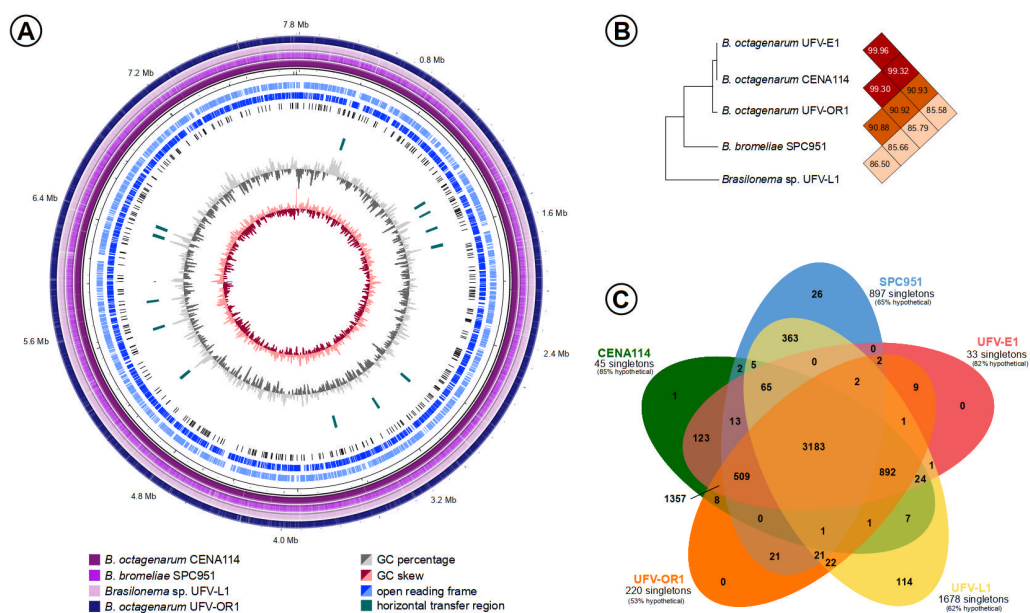
Figure 4 **Comparisons between the *Brasilonema* genomes characterized in this work.** (A) Circular map of the nearly complete genome of *B. octagenarum* UFV-E1 compared to the other *Brasilonema* genomes indicating regions with possible origin by horizontal transfer. (B) Percentages of average nucleotide identities shared between the *Brasilonema* genomes obtained. (C) Quantification of protein clusters orthologous between *Brasilonema* strains and estimation of the amount of singletons encoded in the analyzed genomes.

Full-size 🔲 DOI: 10.7717/peerj.9158/fig-4

sequences present transmembrane domains (Table 4). This suggests that a considerable number of yet uncharacterized proteins are exported from the cells, with some of them possibly involved in ecological interactions.

In accordance with the latest system of cyanobacterial classification by *Komárek et al. (2014)*, the phylogenomic analysis showed that the *Brasilonema* strains were closely related to *Scytonema* representatives, thus confirming previous polyphasic descriptions of the family Scytonemataceae, which in turn clustered inside the order Nostocales (Fig. 6), as expected based on previous works on the taxonomic positioning of these cyanobacteria (*Fiore et al., 2007*; *Komárek et al., 2014*).

Evaluation of sequences that might be involved in plant interactions

Twenty five secondary metabolite gene clusters were predicted in the nearly complete genomes of strains UFV-E1 and CENA114, including clusters encoding the pathways for polyketides, non-ribosomal peptides, post-translationally-modified peptides, bacteriocins, terpenes, indoles, and phenazines, most of which presented low similarity to reference clusters involved in the biosynthesis of known molecules. Five gene clusters, however, presented 100% similarity to references for clusters that encode the biosynthesis of the cyclic non-ribosomal peptides anabaenopeptin and nostopeptolide, the sesquiterpene geosmin, the polyketide 1-heptadecene, and the UV-protecting amino acid shinorine.

Table 3 Genomic features of the *Brasilonema* spp. strains characterized in this work.

Feature	UFV-E1	CENA114	UFV-OR1	SPC 951	UFV-L1
completeness (%)	99.52	100.00	99.28	90.48	99.40
contamination (%)	2.89	2.17	3.01	2.37	1.20
total size (bp)	8,258,380	8,226,398	8,094,337	6,277,767	8,321,598
–chromosome	7,816,330	7,782,641	—	—	—
–plasmid 1	251,877	252,036	—	—	—
–plasmid 2	190,173	191,721	—	—	—
coding sequences (bp)	6,559,505	6,529,766	6,271,238	4,742,865	6,443,634
–chromosome	6,198,811	6,170,908	—	—	—
–plasmid 1	204,544	204,193	—	—	—
–plasmid 2	156,150	154,665	—	—	—
GC content (%)	42.49	42.50	42.48	42.97	41.97
genes	6,950	6,929	6,908	5,693	7,214
protein-coding genes	6,395	6,371	6,309	5,207	6,652
pseudogenes	497	502	541	432	516
RNA genes	58	56	58	54	46
ncRNA	4	4	4	4	4
genes with assigned subsystems	1,394	1,388	1,427	1,137	1,397
genes assigned to COG categories with known function	3,440	3,426	3,379	2,741	3,389
hypothetical proteins	2,081	2,092	2,074	1,695	2,314

Similarity to references for the biosynthesis of known cyanotoxins, which might be involved in plant-pathogen interactions, was not found in any of the assembled genomes.

Annotations in all the *Brasilonema* genomes uncovered several genes encoding enzymes that likely have cellulose, lignin and xylan as substrates (Table 5), which may therefore have a role on leaf colonization and interact with host cell walls. Other enzymes that might have some role during plant colonization have also been annotated in the genomes of all the *Brasilonema* strains, including proteins involved in chitin and protein degradation, auxin biosynthesis and biofilm formation through exopolysaccharide biosynthesis (Table 6).

Protein sequences with similarity to relevant virulence factors from plant pathogens deposited in the Pathogen Host Interaction database were found encoded in the genomes of all five *Brasilonema* strains analyzed in the present work (Table 7). Similarities were found with proteins from phytopathogenic bacteria (*Burkholderia glumae*, *Erwinia amylovora*, *Pantoea ananatis*, *Ralstonia solanacearum*, *Xanthomonas campestris*, *X. citri* and *X. oryzae*), fungi (*Botrytis cinerea*, *Colletotrichum lagenaria*, *Fusarium graminearum*, *F. oxysporum*, *Magnaporthe oryzae* and *Parastagonospora nodorum*) and nematodes (*Bursaphelenchus xylophilus*), which target leaves, shoots, roots, cones, panicles, seedlings, cotyledons or fruits. Among the set of virulence factors with homologous sequences in the *Brasilonema* genomes (36 proteins), the majority (26 proteins) can be considered essential to phytopathogenicity
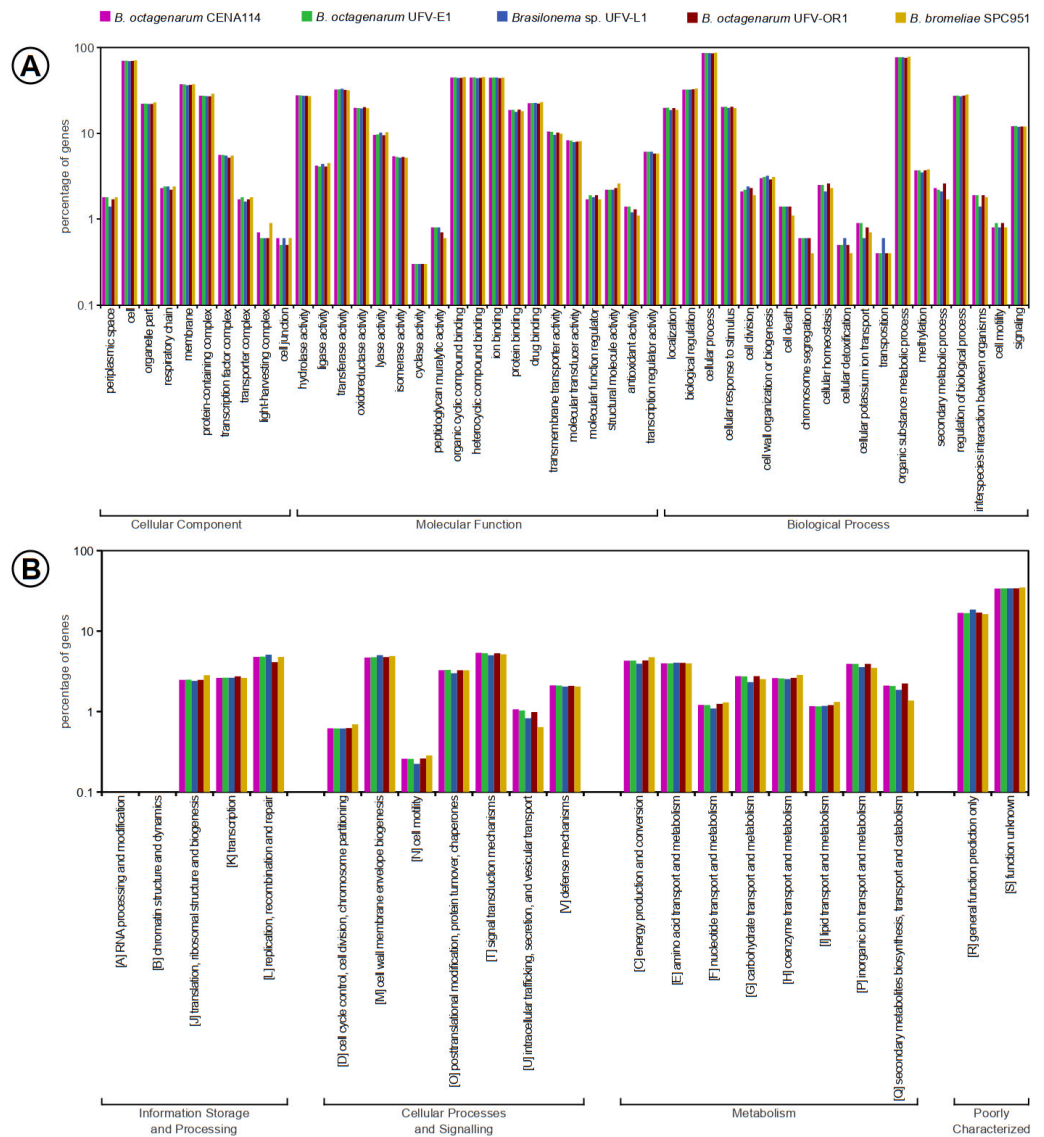
Figure 5 Functional annotations of genes included in the *Brasilonema* spp. genomes characterized in this work, evidencing high similarity between strains and species in this genus. (A) Gene Ontology terms associated with the predicted properties of the products encoded in *Brasilonema* genomes. (B) Distribution of COG categories among *Brasilonema* genomes, showing that they encode a large number of poorly characterized proteins. COG categories W, Y, and Z did not present any matches and thus were suppressed.

Full-size ☑ DOI: 10.7717/peerj.9158/fig-5

since the virulence of the organisms that express these factors may be reduced or even lost after deleterious mutations occur in their coding sequences (Table 7).

It is noteworthy that both nearly complete *B. octagenarum* genomes presented regions with content showing divergent composition when compared to their average content, which is commonly found in horizontally-acquired sequences, while further evidences of horizontal transfer were obtained by predictions of other mobile genetic elements (Fig. 4A).

Table 4 Domains predicted from hypothetical protein sequences encoded in *Brasilonema* genomes.

Strain	Cytoplasmic	Non cytoplasmic	Non cytoplasmic + signal peptide	Cytoplasmic + non cytoplasmic + transmembrane	Cytoplasmic + non cytoplasmic + transmembrane + signal peptide
B. octagenarum UFV-E1	98	1,200	324	417	42
B. octagenarum CENA114	96	1,206	329	415	44
B. octagenarum UFV-OR1	99	1,195	313	399	42
B. bromeliae SPC 951	83	1,019	204	316	44
Brasilonema sp. UFV-L1	140	1,410	278	416	50
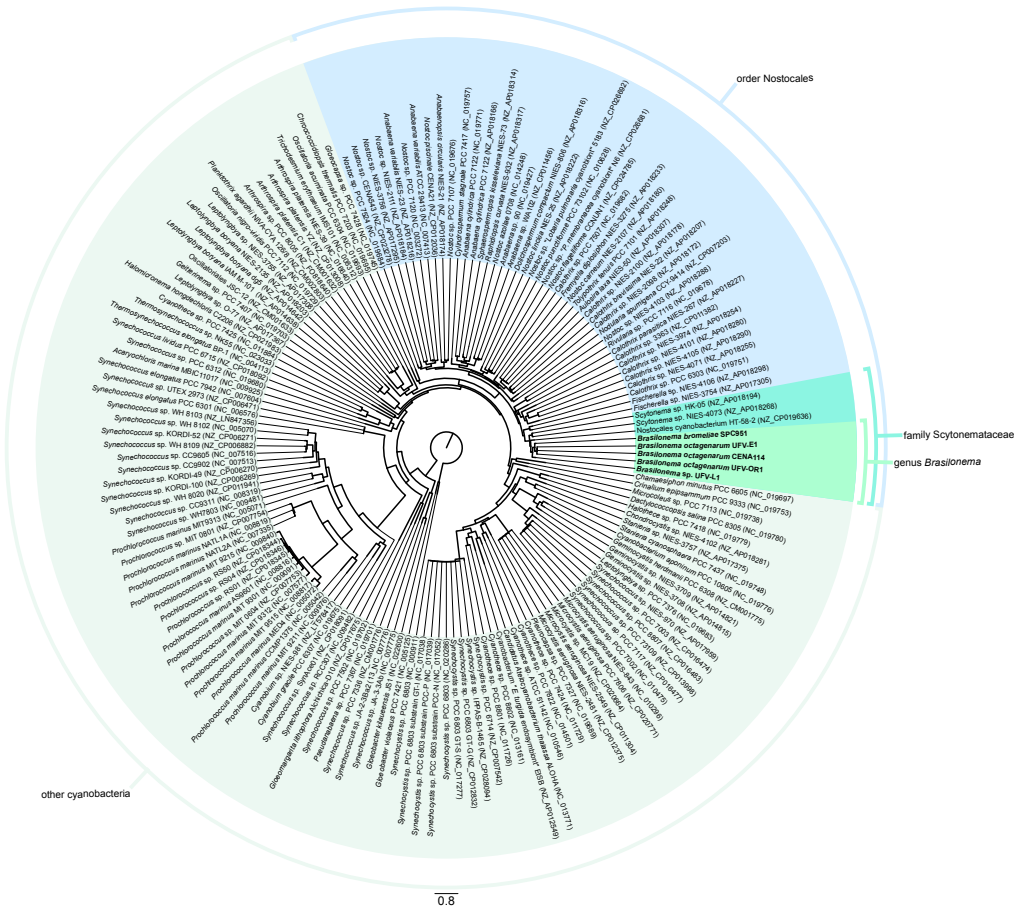
Figure 6 Phylogenomic tree reconstructed by maximum likelihood. Analysis based on alignments of sequences of the 16S rRNA gene and sixty proteins codified in single-copy genes present in the genomes from the strains evaluated in the present work (highlighted in bold) and nearly complete cyanobacterial genomes and chromosome scaffolds from the NCBI RefSeq database.

Full-size ◨ DOI: 10.7717/peerj.9158/fig-6

However, none of the sequences similar to known virulence factors in the *Brasilonema* genomes were found within regions estimated as originating from horizontal transfer, and thus these genes are unlikely to be of xenologous origin.

Table 5 Annotations for enzymes encoded in *Brasilonema* genomes potentially having plant polysaccharides as substrates.

Protein	Substrate	UFV-E1	CENA114	UFV-OR1	SPC 951	UFV-L1
cellulase M	cellulose	+	+	+	+	+
1,4-beta-glucanase / beta-1,4-glucanase	cellulose	+	+	+	+	+
endo-1,4-beta-glucanase	cellulose	+	+	+	+	+
endo-1,4-beta-glucanase E1 precursor	cellulose	+	+	+	+	+
endo-1,4-beta-xylanase	xylan	+	+	+	+	+
endo-1,4-beta-xylanase Z precursor	xylan	+	+	+	+	+
alpha-glucosidase	glucoside	+	+	+	+	+
beta-glucosidase / beta-fucosidase	glucoside / fucoside	+	+	+	–	–
6-fosfo-beta-glucosidase / beta-galactosidase	glucoside / galactoside	+	+	+	–	+
malto-oligosyltrehalose trehalohydrolase	malto-oligosyltrehalose	+	+	+	–	–
4-carboxymuconolactone decarboxylase/alkylhydroperoxidase	lignin	+	+	+	–	+
catalase KatE	lignin	–	–	–	+	+
catalase-peroxidase KatG	lignin	+	+	+	–	–
catalase-like hemeprotein	lignin	+	+	+	+	+
manganese catalase	lignin	+	+	+	+	+
dye-decoloring peroxidase	lignin	+	+	+	–	–
Bcp-type thiol peroxidase	lignin	+	+	+	+	+
alpha-amylase / alpha-manosidase	starch	+	+	+	+	+

DISCUSSION

The initial growth of *B. octagenarum* on the surface of *E. urograndis* leaves apparently occurred as a relationship of epiphytism, as no detrimental effects to the host plant were initially observed. *B. octagenarum* colonization of *E. urograndis* later provided benefits to the host, which was evidenced by the higher production of root and stem dry mass in comparison to the control group (Table 2). The production and release of plant growth regulators by cyanobacteria has been confirmed in several studies with the identification of abscisic acid, auxins, cytokinins, ethylene and gibberelins (*Singh et al., 2017*), and stimulus to plant growth caused by cyanobacteria has been observed when these microorganisms are used as biofertilizers (*Jhala, Panpatte & Vyas, 2017*; *Muñoz Rojas et al., 2018*). Therefore, it is likely that colonization by cyanobacteria stimulated the growth of the host plants by the release of plant growth regulators by *B. octagenarum*.

On the other hand, the consequential decrease in the Chl *a*/*b* ratio in leaves resulting in the lighter green areas observed in Fig. 2 is most likely a direct response to the decrease in light incidence caused by sunlight blockage by the epiphyllic cyanobacterial colonies. Chl *a*/*b* ratio tends to decrease in response to shading, as previously observed in experiments with decreased light incidence in *Tetrastigma hemsleyanum* (*Dai et al., 2009*). This likely represents the early stages of leaf damage by the cyanobacterium and could lead to more severe consequences to the host plant in case of prolonged exposure. As described by *Aguiar et al. (2008)*, in plants that remain for long periods under nursery conditions favorable to the development of microbial mats, extended cyanobacterial colonization starts to act as a

Table 6 Proteins encoded in the genomes of *Brasilonema* spp. strains presenting functional predictions previously described as involved in plant-infection processes.

Protein	Function	UFV-E1	CENA114	UFV-OR1	SPC 951	UFV-L1
glucosamine-6-phosphate deaminase	chitin degradation	+	+	+	+	+
N-acetylglucosamine-6-phosphate deacetylase	chitin degradation	+	+	+	+	+
N-acetylglucosamine kinase	chitin degradation	+	+	+	−	+
N-acetylglucosamine-related transporter NagX	chitin degradation	+	+	+	+	+
ClpP class periplasmic serine protease	protein degradation	+	+	+	+	+
serine protease	protein degradation	+	+	+	+	+
rhomboid family serine protease	protein degradation	+	+	+	+	+
serpin family serine protease inhibitor	protein degradation	+	+	+	+	+
anthranilate phosphoribosyltransferase	auxin biosynthesis	+	+	+	+	+
phosphoribosylanthranilate isomerase	auxin biosynthesis	+	+	+	+	+
aromatic L-amino acid decarboxylase	auxin biosynthesis	+	+	+	−	+
indole-3-pyruvate decarboxylase	auxin biosynthesis	+	+	+	−	−
tryptophan synthase –alpha chain	auxin biosynthesis	+	+	+	+	+
tryptophan synthase –beta chain	auxin biosynthesis	+	+	+	+	+
auxin efflux carrier protein	auxin biosynthesis	+	+	+	+	+
exopolysaccharide synthesis protein	exopolysaccharide biosynthesis	+	+	+	−	+
exopolysaccharide production protein ExoZ	exopolysaccharide biosynthesis	+	+	+	+	+
exopolysaccharide production protein ExoQ	exopolysaccharide biosynthesis	+	+	+	−	+
Hop protein	type III secretion system effector	+	+	+	+	+

stress factor compromising the source/drain balance of eucalyptus plants and could result in necrosis.

Overall, the *Brasilonema* protein sequences that presented similarity to sequences in PHI-base could perform roles in diverse molecular mechanisms such as biosynthesis and degradation, transport, signaling, regulation, starvation response, reproduction, motility and other processes, including currently unknown functions. Ten matches between the translated protein sequences from the *Brasilonema* genomes and proteins deposited in PHI-base (C5A9K4, D4I307, F5HCK8, G4ML75, G4MTK2, Q4UTV7, Q4UUL4, Q8XSV8, Q8Y0J2 and Q9C1T0) are likely to indicate enzymes with roles in primary metabolism (*Cooley et al., 1999*; *Namiki et al., 2007*; *O'Connell et al., 2013*; *Karki & Ham, 2014*; *Ramos et al., 2014*; *Feng et al., 2015*; *Saint-Macary et al., 2015*; *Zhang et al., 2015a*). Since mutants for the inactivation of the genes that encode their homologues in pathogens usually present auxotrophy, the presence of genes for proteins homologous to those factors in the *Brasilonema* genomes does not necessarily reflect any additional capacity of these strains to colonize plant surfaces. Additionally, a number of sequences in the *Brasilonema* genomes have presented similarity with polyketide synthases of unknown functions deposited in PHI-base (UniProt accession numbers I1RSU2, Q6RKH3, Q6RKH4 and Q6RKH5), but since the inactivation of the genes encoding these enzymes have not affected pathogenicity, it is unlikely that their homologues in *Brasilonema* genomes have roles in plant colonization. Four sequences from the UFV-E1 genome matched proteins that have been described as part of two-component systems involved in pathogenic

Table 7 Virulence factors synthesized by phytopathogens with similarity to proteins encoded in *Brasilonema* genomes. An expanded version of this table is provided as Table S1.

UniProt accession	Protein	Function	UFV-E1	CENA114	UFV-OR1	SPC 951	UFV-L1
A0A0K0GHK1	SreR	two-component system regulation	+	+	+	+	+
A0A0K0GI30	DetR	two-component system cytoplasmic signaling	+	+	+	+	+
A0A0U1YU79	PilT	twitching motility	+	+	+	+	+
A4K9H6	PhoP	two-component system regulation	+	+	+	+	+
A4QUT2	CPXB	catalase-peroxidase	+	+	+	–	–
B0LFQ7	Bx-Prx	reproduction and pathogenicity	+	+	+	+	+
C5A846	PidR	two-component system regulation	+	+	+	+	+
C5A9K4	AroB	3-dehydroquinate synthase	+	+	+	–	+
D4HUY4	YhbH	ribosome-associated modulation protein	+	+	+	+	+
D4HX24	RpoS	regulation of stress and starvation response	–	–	–	+	+
D4HXR8	AcrD	resistance-nodulation-cell division transport	+	+	+	+	+
D4I307	ArgD	N-acetylornithine aminotransferase	+	+	–	–	+
F5HCK8	IPMDH	3-isopropylmalate dehydrogenase	+	+	+	+	+
G4ML75	MET6	methyltetrahydropteroyltriglutamate-homocysteine S-methyltransferase	+	+	+	–	–
G4MTK2	MoARG1	arginine biosynthesis	+	+	+	+	+
G4MXC5	MoPRX1	peroxiredoxin peroxidase	+	+	+	+	+
G4N4N6	MoSFA1	S-(hydroxymethyl)glutathione dehydrogenase	+	+	+	+	+
G4NCL5	MGG_00383	hypothetical protein	+	+	+	+	+
I1RSU2	PKS9/KSA1	polyketide synthase	+	+	+	+	–
P87025	THR1	reductase	–	–	–	+	+
Q12634	BUF/BUF1	undefined	+	+	+	+	+
Q2LK92	BcPIC5/BcFKBP12	rapamycin sensitivity	+	+	+	+	+
Q4UQD0	XC_3703	cyclic di-GMP effector	+	+	+	–	+
Q4UTV7	XC_2466	aspartate alpha-decarboxylase	+	+	+	+	+
Q4UUL4	XC_2203	nucleotide diphosphate kinase	+	+	+	+	+
Q58PW8	HsvA	hrp-associated systemic virulence	–	–	–	–	+
Q5H3K9	ColR	undefined	+	+	+	+	+
Q6RKH3	PKS7	polyketide synthase	+	+	+	–	+
Q6RKH4	PKS6	polyketide synthase	+	+	+	–	+
Q6RKH5	PKS5	polyketide synthase	+	+	+	–	–
Q7WTQ9	AcrB	multidrug efflux pump	+	+	+	+	+
Q8PM59	PstB	phosphate metabolism	+	+	+	+	+
Q8XSV8	FabG2	3-ketoacyl-acyl carrier protein reductase	+	+	+	+	+
Q8Y0J2	FabG1	3-ketoacyl-acyl carrier protein reductase	+	+	+	+	+

Table 7 (*continued*)

UniProt accession	Protein	Function	UFV-E1	CENA114	UFV-OR1	SPC 951	UFV-L1
Q9C1T0	ARG1	argininosuccinate lyase	+	+	+	+	+
Q9UWF0	CAM	undefined	−	−	−	−	+

processes (accessions A0A0K0GHK1, A0A0K0GI30, A4K9H6 and C5A846), but since two-component systems control behavior not only during pathogenicity, but also in cell communication and environmental adaptation (*Zschiedrich, Keidel & Szurmant, 2016*), these proteins might also have biological roles other than plant colonization.

The remaining protein sequences with similarity to PHI-base entries could have important roles for plant colonization. Five *Brasilonema* sequences have presented similarity with proteins involved in regulatory cascades for virulence (D4HUY4, D4HX24, Q4UQD0, Q58PW8 and Q5H3K9) (*Oh, Kim & Beer, 2005*; *Subramoni et al., 2012*; *An et al., 2014*; *Ancona, Li & Zhao, 2014*; *Santander et al., 2014*). Two hypothetical proteins from PHI-base (G4NCL5 and Q2LK92) presenting similarity to *Brasilonema* sequences were previously shown to have significant effects on plant pathogenicity, including severe symptoms like necrosis (*Gioti et al., 2006*; *Jeon et al., 2007*). Three copies of the twitching motility gene *pilT* were annotated in the UFV-E1 genome, important for spreading pathogen cells on the surface of the host (*Weller-Stuart et al., 2017*). Three translated protein sequences from the UFV-E1 genome have shown similarity with catalase-peroxidases and peroxiredoxins from PHI-base (accessions A4QUT2, B0LFQ7 and G4MXC5), enzymes with very important roles in the maintenance of redox homeostasis and the protection of pathogen cells from oxidative damage brought by hydrogen peroxide produced by host cells (*Tanabe et al., 2011*; *Fu et al., 2014*; *Mir et al., 2015*; *Santander, Figàs-Segura & Biosca, 2018*). Genes for other proteins potentially involved in detoxification have also been predicted, including multidrug efflux pumps (D4HXR8 and Q7WTQ9), which may confer resistance to phytoalexins (*Burse, Weingart & Ullrich, 2004*), and S-(hydroxymethyl)gluthatione dehydrogenase (G4N4N6), which is produced by phytopathogens as protection against damage from nitric oxide (*Zhang et al., 2015b*).

Although the identification of sequences similar to virulence factors in the *Brasilonema* genomes represents a potential for these cyanobacteria to cause damage to plants, their role within *Brasilonema* interactions with their hosts warrants further functional studies for the evaluation of the conditions under which these genes can be expressed. Nevertheless, except for one gene encoding a putative secreted protein that is likely a distant homolog of the Hop effector protein (Table 5), which is also found in other cyanobacteria with a presumed function of kinase (*Zhang et al., 2016*), the type III secretion system as well as its effectors appear to be completely absent in the assembled *Brasilonema* genomes. This is in agreement with observations for other cyanobacteria showing that they present the types I, II and IV secretion systems, but not the type III (*Gonçalves et al., 2019*). Since the transmission of this secretion system can occur either by vertical or horizontal transfer (*Jackson et al., 2011*), its absence in *Brasilonema* spp. together with the lack of evidence for horizontal transfer in the encoding of other molecules provides further evidence that

leaf damage in this species emerged independently and not from the acquisition of genetic material from plant pathogens.

The role of type III secretion systems together with cell wall-degrading enzymes, serine proteases, phytohormones, siderophores and exopolysaccharides, among other molecules, has been increasingly recognized in plant pathogenesis (*Lindeberg, 2012*; *Melotto & Kunkel, 2013*). Most phytopathogens that affect plant productivity (including species of *Xanthomonas*, *Pseudomonas*, *Agrobacterium*, *Ralstonia* and *Erwinia*) are gram-negative, as are cyanobacteria, and one of the main mechanisms of virulence and pathogenicity of these phytopathogens is the type III secretion system, through which effector proteins are injected into host tissues, bringing about several functions that promote pathogenic processes (*Sherif et al., 2015*). Consequently, even if potential virulence factors, plant cell wall-degrading enzymes and other molecules were produced by the cyanobacteria in contact with their hosts, the absence of the type III secretion system in *Brasilonema* spp. is therefore a great obstacle for these microbes to actively infect plant cells.

CONCLUSIONS

Brasilonema octagenarum UFV-E1 efficient growth and colonization of the phyllosphere was shown to cause lighter green areas on *Eucalyptus urograndis* leaves as a result of the decrease in the Chl *a/b* ratio. Sequences similar to known virulence factors from phytopathogens were found not only in the genome of *B. octagenarum* UFV-E1, originally isolated from damaged *E. urograndis* leaves, but also in the genome of *B. octagenarum* UFV-OR1, isolated from orchid leaves but not reported as causing damage to its host. However, none of these sequences were located within horizontally transferred regions, suggesting that horizontal gene transfer did not play a significant role in the emergence of the capacity for damaging leaves by *Brasilonema*. If these proteins also act as virulence factors, leaf damage by this species may be either restricted in host range or triggered by a more complex, uncommon set of factors making it a phenomenon of rare occurrence and thus not commonly observed. Similar sequences were also found in the genomes of *B. octagenarum* CENA114, obtained from a wet iron water pipe, *B. bromeliae* SPC 951 and *Brasilonema* sp. UFV-L1, isolated respectively from bromeliad and ligustrum leaves, which could suggest that the potential for leaf damage is not restricted to a single phyllosphere species, but also present in *Brasilonema* strains from other habitats and species.

Nevertheless, it is unlikely that these cyanobacteria could be capable of injecting any virulence factors and effectors into their plant hosts considering that the type III secretion system is the main vehicle of infection in known phytopathogenic bacteria but it is absent in this genus. Therefore, even if virulence factors could be expressed by the cyanobacteria in contact with plants, they appear to have no way of reaching the cytoplasm of their hosts since their genomes do not encode the structural proteins necessary for this process. This makes damage by *B. octagenarum* largely an indirect consequence of the growth of cyanobacterial mats on the leaf surface, causing the blockage of sunlight and hindering photosynthesis by the host, which could possibly progress into more severe consequences after extended colonization. It is therefore possible that other epiphyllic cyanobacteria,

even those that do not produce any potential virulence factors, also cause similar damage if specific environmental conditions allow for their biomass to achieve significant volume. Consequently, even though epiphyllic cyanobacteria are traditionally thought of as being universally beneficial to their hosts, benefits to plants may come at a cost that may outbalance them when certain conditions that greatly favor cyanobacterial growth are met.

ACKNOWLEDGEMENTS

ADDITIONAL INFORMATION AND DECLARATIONS

Competing Interests

The authors declare there are no competing interests.

Author Contributions

- Danillo O. Alvarenga and Maione W. Franco conceived and designed the experiments, performed the experiments, analyzed the data, prepared figures and/or tables, authored or reviewed drafts of the paper, and approved the final draft.
- Kaarina Sivonen analyzed the data, authored or reviewed drafts of the paper, and approved the final draft.
- Marli F. Fiore conceived and designed the experiments, analyzed the data, authored or reviewed drafts of the paper, and approved the final draft.
- Alessandro M. Varani conceived and designed the experiments, performed the experiments, analyzed the data, prepared figures and/or tables, authored or reviewed drafts of the paper, and approved the final draft.

Data Availability

The following information was supplied regarding data availability:

The sequences are available at GenBank: CP030118–CP030123, QMEA00000000, QMEB00000000, QMEC00000000.

Supplemental Information

Supplemental information for this article can be found online at http://dx.doi.org/10.7717/peerj.9158#supplemental-information.

REFERENCES

Adams DG, Bergman B, Nierzwicki-Bauer SA, Rai AN, Schüssler A. 2013. Cyanobacterial plant symbioses. In: Rosenberg E, DeLong EF, Stackebrandt E, Lory S, Thompson F, eds. *The prokaryotes: prokaryotic biology and symbiotic associations*. Berlin: Springer-Verlag, 359–400.

Aguiar R, Fiore MF, Franco MW, Ventrella MC, Lorenzi AS, Vanetti CA, Alfenas AC. 2008. A novel epiphytic cyanobacterial species from the genus *Brasilonema* causing damage to *Eucalyptus* leaves. *Journal of Phycology* **44**:1322–1334 DOI 10.1111/j.1529-8817.2008.00584.x.

Akhter S, Aziz RK, Edwards RA. 2012. PhiSphy: a novel algorithm for finding prophages in bacterial genomes that combines similarity- and composition-based strategies. *Nucleic Acids Research* **40**:e126 DOI 10.1093/nar/gks406.

Allen MM. 1968. Simple conditions for growth of unicellular blue–green algae on plates. *Journal of Phycology* **4**:1–4 DOI 10.1111/j.1529-8817.1968.tb04667.x.

Alvarenga DO, Moreira LM, Chandler M, Varani AM. 2018. A practical guide for comparative genomics of mobile genetic elements in prokaryotic genomes. In: Setubal JC, Stoye PF, Stadler PF, eds. *Methods in molecular biology 1704: comparative genomics*. New York: Humana Press, 213–242.

An S, Carly DL, McCarthy Y, Murdoch SL, Ward J, Febrer M, Dow JM, Ryan RP. 2014. Novel cyclic di-GMP effectors of the YajQ protein family control bacterial virulence. *PLOS ONE* **10**:e1004429 DOI 10.1371/journal.ppat.1004429.

Ancona V, Li W, Zhao Y. 2014. Alternative sigma factor RpoN and its modulation protein YhbH are indispensable for *Erwinia amylovora* virulence. Molecular. *Molecular Plant Pathology* **15**:58–66 DOI 10.1111/mpp.12065.

Bankevich A, Nurk S, Antipov D, Grevich AA, Dvorkin M, Kulikov A, Lesin VM, Nikolenko SI, Pham S, Prjibelski AD, Pyshkin AV, Sirotkin AV, Vyahhi N, Tesler G, Alekseyev MA, Pevzner PA. 2012. SPAdes: a new genome assembly algorithm and its applications to single-cell sequencing. *Jornal of Computational Biology* **19**:455–477 DOI 10.1089/cmb.2012.0021.

Becerra-Absalón I, Rodarte B, Osorio K, Alba-Lois L, Segal-Kischinevzky C, Montejano G. 2013. A new species of *Brasilonema* (Scytonemataceae, Cyanoprokaryota) from Tolantongo, Hidalgo, Central Mexico. *Fottea* **13**:25–38 DOI 10.5507/fot.2013.003.

Bengtsson J, Eriksson KM, Hartmann M, Wang Z, Shenoy BD, Grelet GA, Abarenkov K, Petri A, Rosenblad MA, Nilsson RH. 2011. Metaxa: a software tool for automated detection and discrimination among ribosomal small subunit (12S/16S/18S) sequences of archaea, bacteria, eukaryotes, mitochondria, and chloroplasts in metagenomes and environmental sequencing datasets. *Antonie van Leeuwenhoek* **100**:471 DOI 10.1007/s10482-011-9598-6.

Bolger AM, Lohse M, Usadel B. 2014. Trimmomatic: a flexible trimmer for Illumina sequence data. *Bioinformatics* **30**:2114–2120 DOI 10.1093/bioinformatics/btu170.

Brettin T, Davis JJ, Disz T, Edwards RA, Gerdes S, Olsen GJ, Olson R, Overbeek R, Parrello B, Pusch GD, Shukla M, 3rd ThomasonJA, Stevens R, Vonstein V, AR7 Wattam, Xia F. 2015. RASTtk: a modular and extensible implementation of the RAST algorithm for building custom annotation pipelines and annotating batches of genomes. *Scientific Reports* **5**:8365 DOI 10.1038/srep08365.

Bukatsch F. 1972. Bemerkungen zur doppelfärbung astrablau-safranin. *Mikrokosmos* **61**:255.

Burse A, Weingart H, Ullrich MS. 2004. The phytoalexin-inducible multidrug efflux pump AcrAB contributes to virulence in the fire blight pathogen, *Erwinia amylovora*. *Molecular Plant Microbe Interactions* **17**:43–54 DOI 10.1094/MPMI.2004.17.1.43.

Camacho C, Coulouris G, Avagyan V, Ma N, Papadopoulos J, Bealer K, Madden TL. 2009. BLAST+: architecture and applications. *BMC Bioinformatics* **10**:421 DOI 10.1186/1471-2105-10-421.

Carver T, Harris SR, Berriman M, Parkhill J, McQuillan JA. 2012. Artemis: an integrated platform for visualization and analysis of high-throughput sequence-based experimental data. *Bioinformatics* **15**:464–469 DOI 10.1093/bioinformatics/btr703.

Cooley RN, Monk TP, McLoughlin SB, Foster SG, Dancer JE. 1999. Gene disruption and biochemical characterisation of 3-isopropylmalate dehydrogenase from *Stagonospora nodorum*. *Pesticide Science* **55**:364–367 DOI 10.1002/(SICI)1096-9063(199903)55:3<364::AID-PS910>3.0.CO;2-K.

Dai Y, Shen Z, Liu Y, Wang L, Hannaway D, Lu H. 2009. Effects of shade treatment on the photosynthetic capacity, chlorophyll fluorescence, and chlorophyll content of *Tetrastigma hemsleyanum* Diels et Gilg. *Environmental and Experimental Botany* **65**:177–182 DOI 10.1016/j.envexpbot.2008.12.008.

Edgar RC. 2010. Search and clustering orders of magnitude faster than BLAST. *Bioinformatics* **26**:2460–2461 DOI 10.1093/bioinformatics/btq461.

Eichinger V, Nussbaumer T, Platzer A, Jehl MA, Arnold R, Rattei T. 2016. Effective DB–updates and novel features for a better annotation of bacterial secreted proteins and type III, IV, VI secretion systems. *Nucleic Acids Research* **44**:D669–D674 DOI 10.1093/nar/gkv1269.

Feng SX, Ma JC, Yang J, Hu Z, Zhu L, Bi HK, Sun YR, Wang HH. 2015. *Ralstonia solanacearum* fatty acid composition is determined by interaction of two 3-ketoacyl-acyl carrier protein reductases encoded on separate replicons. *BMC Microbiology* **15**:223 DOI 10.1186/s12866-015-0554-x.

Fiore MF, Sant'Anna CL, Azevedo MTP, Komárek J, Kaštovský J, Sulek J, Lorenzi AS. 2007. The cyanobacterial genus *Brasilonema* gen. nov. a molecular and phenotypic evaluation. *Journal of Phycology* **43**:789–798 DOI 10.1111/j.1529-8817.2007.00376.x.

Fu HY, Ren JH, Huang L, Li H, Ye JR. 2014. Screening and functional analysis of the peroxiredoxin specifically expressed in *Bursaphelenchus xylophilus*—the causative agent of pine wilt disease. *International Journal of Molecular Sciences* **15**:10215–20232 DOI 10.3390/ijms150610215.

Ganesan H, Rakitianskaia AS, Davenport CF, Tümmler B, Reva ON. 2008. The SeqWord Genome Browser: an online tool for the identification and visualization of atypical regions of bacterial genomes through oligonucleotide usage. *BMC Bioinformatics* **9**:333 DOI 10.1186/1471-2105-9-333.

Gioti A, Simon A, Pêcheur PLe, Giraud C, Pradier JM, Viaud M, Levis C. 2006. Expression profiling of *Botrytis cinerea* genes identifies three patterns of up-regulation in planta and an FKBP12 protein affecting pathogenicity. *Journal of Molecular Biology* **358**:372–386 DOI 10.1016/j.jmb.2006.01.076.

Gonçalves CF, Lima S, Tamagnini P, Oliveira P. 2019. Cyanobacterial secretion systems: understanding fundamental mechanisms toward technological applications. In: Mishra AK, Tiwari DN, Rai AN, eds. *Cyanobacteria*. London: Academic Press, 359–381.

Götz S, García-Gómez JM, Terol J, Williams TD, Nagaraj SH, Nueda MJ, Robles M, Talón M, Dopazo J, Conesa A. 2008. High-throughput funcional annotation and data mining with the Blast2GO suite. *Nucleic Acids Research* **36**:3420–3435 DOI 10.1093/nar/gkn176.

Hauer T. 2010. Phototrophic biofilms on the interior walls of concrete Iterson-type cooling towers. *Journal of Applied Phycology* **22**:733–736 DOI 10.1007/s10811-010-9513-y.

Huerta-Cepas J, Szklarczyk D, Forslund K, Cook H, Heller D, Walter MC, Rattei T, Mende DR, Sunagawa S, Kuhn M, Jensen LJ, Von Mering C, Bork P. 2016. eggNOG 4.5.1: a hierarchical orthology framework with improved annotations for eukaryotic, prokaryotic and viral sequences. *Nucleic Acids Research* **44**:D286–D293 DOI 10.1093/nar/gkv1248.

Jackson RW, Vinatzer B, Arnold DL, Dorus S, Murillo J. 2011. The influence of the accessory genome on bacterial pathogen evolution. *Mobile Genetic Elements* **1**:55–65 DOI 10.4161/mge.1.1.16432.

Jeon J, Park SY, Chi MH, Choi J, Park J, Rho HS, Kim S, Goh J, Yoo S, Choi J, Park JY, Yi M, Yang S, Kwon MJ, Han SS, Kim BR, Khang CH, Park B, Lim SE, Jung K, Kong S, Karunakaran M, Oh HS, Kim H, Kim S, Park J, Kang S, Choi WB, Kang S, Lee YH. 2007. Genome-wide functional analysis of pathogenicity genes in the rice blast fungus. *Nature Genetics* **39**:561–565 DOI 10.1038/ng2002.

Jhala YK, Panpatte DG, Vyas RV. 2017. Cyanobacteria: source of organic fertilizers for plant growth. In: Panpatte DG, Jhala Y, Vyas R, Shelat H, eds. *Microorganisms for green revolution*. Singapore: Springer, 253–264.

Johansen D. 1940. *Plant microtechnique*. New York: McGraw-Hill.

Kajitani R, Toshimoto K, Noguchi H, Toyoda A, Ogura Y, Okuno M, Yabana M, Harada M, Nagayasu E, Maruyama H, Kohara Y, Fujiyama A, Hayashi T, Itoh T. 2014. Efficient de novo assembly of highly heterozigous genomes from whole-genome shotgun short reads. *Genome Research* **24**:1384–1395 DOI 10.1101/gr.170720.113.

Käll L, Krogh A, Sonnhammer EL. 2007. Advantages of combined transmembrane topology and signal peptide prediction —the Phobius web server. *Nucleic Acids Research* **35**:W429–W432 DOI 10.1093/nar/gkm256.

Kang DD, Froula J, Egan R, Wang Z. 2015. MetaBAT, an efficient tool for accurately reconstructing single genomes from complex microbial communities. *PeerJ* **3**:e1165 DOI 10.7717/peerj.1165.

Karki HS, Ham JH. 2014. The roles of the shikimate pathway genes, *aroA* and *aroB*, in virulence, growth and UV tolerance of *Burkholderia glumae* strain 411gr-6. *Molecular Plant Pathology* **15**:940–947 DOI 10.1111/mpp.12147.

Kaštovský J, Hauer T, Komárek J, Skácelová O. 2010. The list of cyanobacterial species of the Czech Republic to the end of 2009. *Fottea* **10**:245–249 DOI 10.5507/fot.2010.015.

Katoh K, Standley DM. 2013. MAFFT multiple sequence alignment software version 7: improvements in performance and usability. *Molecular Biology and Evolution* **30**:772–780 DOI 10.1093/molbev/mst010.

Komárek J, Kaštovský J, Mareš J, Johansen JR. 2014. Taxonomic classification of cyanoprokaryotes (cyanobacterial genera) 2014, using a polyphasic approach. *Preslia* **86**:295–335.

Lin S, Wu Z, Yu G, Zhu M, Yu B, Li R. 2010. Genetic diversity and molecular phylogeny of *Planktothrix* (Oscillatoriales, Cyanobacteria) strains from China. *Harmful Algae* **9**:87–97 DOI 10.1016/j.hal.2009.08.004.

Lindeberg M. 2012. Genome-enabled perspectives on the composition, evolution, and expression of virulence determinants in bacterial plant pathogens. *Annual Review of Phytopathology* **50**:111–132 DOI 10.1146/annurev-phyto-081211-173022.

Melotto M, Kunkel BN. 2013. Virulence strategies of plant pathogenic bacteria. In: Rosenberg E, DeLong EF, Lory S, Stackebrandt E, Thompson F, eds. *Virulence strategies of plant pathogenic bacteria*. Berlin: Springer-Verlag, 61–82.

Mir AA, Park SY, Sadat MAbu, Kim S, Choi J, Jeon J, Lee YH. 2015. Systematic characterization of the peroxidase gene family provides new insights into fungal pathogenicity in *Magnaporthe oryzae*. *Scientific Reports* **5**:11831 DOI 10.1038/srep11831.

Miscoe LH, Johansen JR, Vaccarino MA, Pietrasiak N, Sherwood AR. 2016. Novel cyanobacteria from caves on Kauai, Hawaii. *Bibliotheca Phycologica* **120**:75–152.

Muñoz Rojas M, Chilton A, Liyanage GS, Erickson TE, Merritt DJ, Neilan BA, Ooi MKJ. 2018. Effects of indigenous soil cyanobacteria on seed germination and seedling growth of arid species used in restoration. *Plant and Soil* **429**:91–100 DOI 10.1007/s11104-018-3607-8.

Namiki F, Matsunaga M, Okuda M, Inoue I, Nishi K, Fujita Y, Tsuge T. 2007. Mutation of an arginine biosynthesis gene causes reduced pathogenicity in *Fusarium oxysporum* f. sp. *melonis*. *Molecular Plant-Microbe Interactions* **14**:580–584 DOI 10.1094/MPMI.2001.14.4.580.

O'Connell A, An SQ, McCarthy Y, Schulte F, Niehaus K, He YQ, Tang JL, Ryan RP, Dow JM. 2013. Proteomics analysis of the regulatory role of Rpf/DSF cell-to-cell signaling system in the virulence of *Xanthomonas campestris*. *Molecular Plant-Microbe Interactions* **26**:1131–1137 DOI 10.1094/MPMI-05-13-0155-R.

O'Connell J, Schulz-Trieglaff O, Carlson E, Hims MM, Gormley NA, Cox AJ. 2015. NxTrim: optimized trimming of Illumina mate pair reads. *Bioinformatics* **31**:2035–2037 DOI 10.1093/bioinformatics/btv057.

Oh CS, Kim JF, Beer SV. 2005. The Hrp pathogenicity island of *Erwinia amylovora* and identification of three novel genes required for systemic infection. *Molecular Plant Pathology* **6**:125–138 DOI 10.1111/j.1364-3703.2005.00269.x.

O'Leary NA, Wright MW, Brister JR, Ciufo S, Haddad D, McVeigh R, Rajput B, Robbertse B, Smith-White B, Ako-Adjei D, Astashyn A, Badretdin A, Bao Y, Blinkova O, Brover V, Chetvernin V, Choi J, Cox E, Ermolaeva O, Farrell CM, Goldfarb T, Gupta T, Haft D, Hatcher E, Hlavina W, Joardar VS, Kodali VK, Li W, Maglott D, Masterson P, McGarvey KM, Murphy MR, O'Neill K, Pujar S, Rangwala SH, Rausch D, Riddick LD, Schoch C, Shkeda A, Storz SS, Sun H, Thibaud-Nissen F, Tolstoy I, Tully RE, Vatsan AR, Wallin C, Webb D, Wu W, Landrum MJ, Kimchi A, Tatusova T, DiCuccio M, Kitts P, Murphy TD, Pruitt KD. 2016. Reference sequence (RefSeq) database at NCBI: current status, taxonomic expansion, and functional annotation. *Nucleic Acids Research* **44**:D733–D745 DOI 10.1093/nar/gkv1189.

Overbeek R, Olson R, Pusch GD, Olsen GJ, Davis JJ, Disz T, Edwards RA, Gerdes S, Parrello B, Shukla M, Vonstein V, Wattam AR, Xia F, Stevens R. 2014. The SEED and the Rapid Annotation of microbial genomes using Subsystems Technology (RAST). *Nucleic Acids Research* **42**:D206–D214 DOI 10.1093/nar/gkt1226.

Parks DH, Imelfort M, Skennerton CT, Hugenholtz P, Tyson GW. 2014. Assessing the quality of microbial genomes recovered from isolates, single cells, and metagenomes. *Genome Research* **25**:1043–1055 DOI 10.1101/gr.186072.114.

Ramos LS, Lehman BL, Peter KA, McNellis TW. 2014. Mutation of the *Erwinia amylovora* argD gene causes arginine auxotrophy, nonpathogenicity in apples, and reduced virulence in pears. *Applied and Environmental Microbiology* **80**:6739–6749 DOI 10.1128/AEM.02404-14.

Rikkinen J. 2007. Cyanobacteria in terrestrial symbiotic systems. In: Hallenbeck PC, ed. *Modern topics in the phototrophic prokaryotes*. Cham: Springer, 243–294.

Robinson DG, Lee MC, Marx CJ. 2012. OASIS: an automated program for global investigation of bacterial and archaeal insertion sequences. *Nucleic Acids Research* **40**:e174 DOI 10.1093/nar/gks778.

Rodarte B, Becerra-Absalón I, Montejano GA, Osorio-Santos K, Alba-Lois L, León-Tejera H, Segal-Kischinevzky C. 2014. Morphological and molecular characterization of *Brasilonema roberti-lamii* (Cyanophyceae, Nostocales, Scytonemataceae), from Central Mexico. *Phytotaxa* **164**:255–264 DOI 10.11646/phytotaxa.164.4.4.

Roux S, Enault F, Hurwitz BL. 2015. VirSorter: mining viral signal from microbial genomic data. *PeerJ* **3**:e985 DOI 10.7717/peerj.985.

Saint-Macary ME, Barbisan C, Gagey MJ, Frelin O, Beffa R, Lebrun MH, Droux M. 2015. Methionine biosynthesis is essential for infection in the rice blast fungus *Magnaporthe oryzae*. *PLOS ONE* **10**:e0111108 DOI 10.1371/journal.pone.0111108.

Santander RD, Figàs-Segura À, Biosca EG. 2018. *Erwinia amylovora* catalases KatA and KatG are virulence factors and delay the starvation-induced viable but non-culturable (VBNC) response. *Molecular Plant Patholy* **19**:922–934 DOI 10.1111/mpp.12577.

Santander RD, Monte-Serrano M, Rodríguez-Herva JJ, López-Solanilla E, Rodríguez-Palenzuela P, Biosca EG. 2014. Exploring new roles for the *rpoS* gene in the survival and virulence of the fire blight pathogen *Erwinia amylovora*. *FEMS Microbiology Ecology* **90**:895–907 DOI 10.1111/1574-6941.12444.

Sant'Anna CL, Azevedo MTP, Fiore MF, Lorenzi AS, Kaštovský J, Komárek P. 2011. Subgeneric diversity of *Brasilonema* (Cyanobacteria, Scytonemataceae). *Brazilian Journal of Botany* **34**:51–62 DOI 10.1590/S0100-84042011000100006.

Sass JE. 1951. *Botanical microtechnique*. Ames: Iowa State College Press.

Sherif S, El-Sharkawy I, Paliyath G, Jayasankar S. 2015. Molecular insights into plant-phytopathogenic bacteria interactions. *Plant Molecular Biology Reporter* **33**:1116–1130 DOI 10.1007/s11105-014-0822-1.

Siguier P, Perochon J, Lestrade L, Mahillon J, Chandler M. 2006. ISfinder: the reference centre for bacterial insertion sequences. *Nucleic Acids Research* **34**:D32–D36 DOI 10.1093/nar/gkj014.

Siguier P, Varani A, Perochon J, Chandler M. 2012. Exploring bacterial insertion sequences with ISfinder: objectives, uses, and future developments. In: Bigot Y, ed. *Methods in molecular biology 859: mobile genetic elements*. New York: Humana Press, 91–103.

Singh R, Parihar P, Singh M, Bajguz A, Kumar J, Singh S, Singh VP, Prasad SM. 2017. Uncovering potential applications of cyanobacteria and algal metabolites in biology, agriculture and medicine: current status and future prospects. *Frontiers in Microbiology* **8**:515 DOI 10.3389/fmicb.2017.00515.

Stamatakis A. 2014. RAxML version 8: a tool for phylogenetic analysis and post-analysis of large phylogenies. *Bioinformatics* **30**:1312–1313 DOI 10.1093/bioinformatics/btu033.

Stanier RY, Kunisawa R, Mandel M, Cohen-Bazire G. 1971. Purification and properties of unicellular blue–green algae (order Chroococcales). *Bacteriological Reviews* **35**:171–205.

Subramoni S, Pandey A, Vishnu Priya MR, Patel HK, Sonti RV. 2012. The ColRS system of *Xanthomonas oryzae* pv. *oryzae* is required for virulence and growth in iron-limiting conditions. *Molecular Plant Pathology* **13**:690–703 DOI 10.1111/j.1364-3703.2011.00777.x.

Tanabe S, Ishii-Minami N, Saitoh KI, Otake Y, Kaku H, Shibuya N, Nishizawa Y, Minami E. 2011. The Role of catalase-peroxidase secreted by *Magnaporthe oryzae* during early infection of rice cells. *Molecular Plant-Microbe Interactions* **24**:162–171 DOI 10.1094/MPMI-07-10-0175.

Tatusova T, DiCuccio M, Badretdin A, Chetvernin V, Nawrocki EP, Zaslavsky L, Lomsadze A, Pruitt KD, Borodovsky M, Ostell J. 2016. NCBI prokaryotic genome annotation pipeline. *Nucleic Acids Research* **44**:6614–6624 DOI 10.1093/nar/gkw569.

Urban M, Cuzick A, Seager J, Wood V, Rutherford K, Venkatesh SY, De Silva N, Martinez MC, Pedro H, Yates AD, Hassani-Pak K, Hammond-Kosack KE. 2020. PHI-base: the pathogen-host interactions database. *Nucleic Acids Research* **48**:D613–D620 DOI 10.1093/nar/gkz904.

Usher KM, Bergman B, Raven JA. 2007. Exploring cyanobacterial mutualisms. *Annual Review of Ecology, Evolution and Systematics* **38**:255–273 DOI 10.1146/annurev.ecolsys.38.091206.095641.

Vaccarino MA, Johansen JR. 2012. *Brasilonema angustatum* sp.nov. (Nostocales), a new filamentous cyanobacterial species from the Hawaiian islands. *Journal of Phycology* **48**:1178–1186 DOI 10.1111/j.1529-8817.2012.01203.x.

Vernikos GS, Parkhill J. 2006. Interpolated variable order motifs for identification of horizontally acquired DNA: revisiting the *Salmonella* pathogenicity islands. *Bioinformatics* **22**:2196–2203 DOI 10.1093/bioinformatics/btl369.

Villanueva CD, Garvey AD, Hašler P, Dvořák P, Poulíčková A, Norwich AR, Casamatta DA. 2019. Descriptions of *Brasilonema geniculatum* and *Calothrix dumus* (Nostocales, Cyanobacteria): two new taxa isolated from cemetery tombstones. *Phytotaxa* **387**:1–20 DOI 10.11646/phytotaxa.387.1.1.

Villanueva CD, Hašler P, Dvořák P, Poulíčková A, Casamatta DA. 2018. *Brasilonema lichenoides* sp.nov. and *Chroococcidiopsis lichenoides* sp. nov. (Cyanobacteria): two novel cyanobacterial constituents isolated from a tripartite lichen of headstones. *Journal of Phycology* **54**:224–233 DOI 10.1111/jpy.12621.

Wang Y, Coleman-Derr D, Chen G, Gu YQ. 2015. OrthoVenn: a web server for genome wide comparison and annotation of orthologous clusters across multiple species. *Nucleic Acids Research* **43**:W78–W84 DOI 10.1038/nrmicro2910.

Wang Z, Wu M. 2013. A phylum-level bacterial phylogenetic marker database. *Molecular Biology and Evolution* **30**:1258–1262 DOI 10.1093/molbev/mst059.

Wellburn AR. 1994. The spectral determination of chlorophylls *a* and *b*, as well as total carotenoids, using various solvents with spectrophotometers of different resolution. *Journal of Plant Physiology* **144**:307–313 DOI 10.1016/S0176-1617(11)81192-2.

Weller-Stuart T, Toth I, De Maayer P, Coutinho T. 2017. Swimming and twitching motility are essential for attachment and virulence of *Pantoea ananatis* in onion seedlings. *Molecular Plant Pathology* **18**:734–745 DOI 10.1111/mpp.12432.

Wood DE, Salzberg SL. 2014. Kraken: ultrafast metagenomic sequence classification using exact alignments. *Genome Biology* **15**:R46 DOI 10.1186/gb-2014-15-3-r46.

Xie Z, Tang H. 2017. ISEScan: automated identification of insertion sequence elements in prokaryotic genomes. *Bioinformatics* **21**:3340–3347 DOI 10.1093/bioinformatics/btx433.

Ye J, Zhang Y, Cui H, Liu J, Wu Y, Cheng Y, Xu H, Huang X, Li S, Zhou A, Zhang X, Bolund L, Chen Q, Wang J, Yang H, Fang L, Shi C. 2018. WEGO 2.0: a web tool for analyzing and plotting GO annotations, 2018 update. *Nucleic Acids Research* **46**:W71–W75 DOI 10.1093/nar/gky400.

Yoon SH, Ha SM, Lim J, Kwon S, Chun J. 2017. A large-scale evaluation of algorithms to calculate average nucleotide identity. *Antonie van Leeuwenhoek* **110**:1281–1286 DOI 10.1007/s10482-017-0844-4.

Zhang X, Carter MS, Vetting MW, San Francisco B, Zhao S, Al-Obaidi NF, Solbiati JO, Thiaville JJ, De Crécy-Lagard V, Jacobson MP, Almo SC, Gerlt JA. 2016. Assignment of function to a domain of unknown function: DUF1537 is a new kinase family in catabolic pathways for acid sugars. *Proceedings of the National Academy of Sciences of the United States of America* **113**:E4161–E4169 DOI 10.1073/pnas.1605546113.

Zhang Y, Shi H, Liang S, Ning G, Xu N, Lu J, Liu X, Lin F. 2015a. MoARG1, MoARG5, 6 and MoARG7 involved in arginine biosynthesis are essential for growth, conidiogenesis, sexual reproduction, and pathogenicity in *Magnaporthe oryzae*. *Microbiological Research* **180**:11–22 DOI 10.1016/j.micres.2015.07.002.

Zhang Z, Wang J, Chai R, Qiu H, Jiang H, Mao X, Wang Y, Liu F, Sun G. 2015b. An S-(hydroxymethyl)gluthatione dehydrogenase is involved in conidiation and full virulence in the rice blast fungus *Magnaporthe oryzae*. *PLOS ONE* **10**:e0120627 DOI 10.1371/journal.pone.0120627.

Zimin AV, Marçais G, Puiu D, Roberts M, Salzberg SL, Yorke JA. 2013. The MaSuRCA genome assembler. *Bioinformatics* **29**:2669–2677 DOI 10.1093/bioinformatics/btt476.

Zschiedrich CP, Keidel V, Szurmant H. 2016. Molecular mechanisms of two-component signal transduction. *Journal of Molecular Biology* **428**:3752–3775 DOI 10.1016/j.jmb.2016.08.003.